

Synthesis of carboxyl-functionalized 3D macroporous polypyrrole using porogen-free method and its application as a support for the covalent attachment of urease

Edith Mawunya Kutorglo ^{a,†,*}, František Muzika ^a, Fatima Hassouna ^{a,*}, Giuseppe Storti ^b, Dušan Kopecký ^c, Roman Bleha ^d, Andriy Synytsya ^d, Ivona Sedlářová ^e, and Miroslav Šoóš ^{a,*}

^a Department of Chemical Engineering, University of Chemistry and Technology, Technická 3, 166 28 Prague 6 – Dejvice, Czech Republic.

^b Institute for Chemistry and Bioengineering, Department of Chemistry and Applied Biosciences, ETH Zurich, Vladimir-Prelog-Weg 1-5/10, 8093 Zürich, Switzerland.

^c Department of Computing and Control Engineering, University of Chemistry and Technology, Technická 5, 166 28 Prague 6 – Dejvice, Czech Republic.

^d Department of Carbohydrates and Cereals, University of Chemistry and Technology, Technická 3, 166 28 Prague 6 – Dejvice, Czech Republic.

^e Department of Inorganic Technology, University of Chemistry and Technology, Technická 5, 166 28 Prague 6 – Dejvice, Czech Republic.

[†] Current affiliation: Department of Solid State Engineering, University of Chemistry and Technology, Technická 3, 166 28 Prague 6 – Dejvice, Czech Republic

* To whom correspondence should be addressed: miroslav.soos@vscht.cz (M. Šoóš); fatima.hassouna@vscht.cz (F. Hassouna); kutorgle@vscht.cz (E. M. Kutorglo)

Abstract

The immobilization of enzymes onto solid supports is a common strategy for obtaining improved stability, fast ~~simple~~ product separation, enzyme reusability, and, ultimately, lower operating costs. Therefore, the development of new immobilization supports is of significant interest. Herein, stable three-dimensional (3D) macroporous materials were synthesized from polypyrrole by a simple template approach and used as an immobilization support for urease. The template method entails the use of polypyrrole nanoparticle building blocks, onto which a carboxylic acid-functionalized pyrrole monomer was polymerized, forming a 3D macroporous structure with tunable pore size distribution. SEM images, together with static light scattering, revealed the 3D macroporous nature of the materials. The properties of both the macroporous supports and the immobilized enzyme were characterized using a combination of techniques. The ability of the bioconjugated urease to catalyze the hydrolysis of urea into carbon dioxide and ammonia was then tested. The immobilized enzyme exhibited good catalytic activity, stability and reusability. Overall, these results suggest that such 3D macroporous materials with chemically accessible surfaces have considerable potential for use as biocatalyst supports.

Keywords: Polypyrrole, Urease, Three-dimensional, Macroporous support, Enzymatic catalysis, Bioconjugation, Immobilization

1 Introduction

Many industrial processes and component technologies, including medical diagnostics, water treatment, biocatalysis and separation, rely on enzymes or other biomolecules suspended in a reaction mixture [1]. Usually, the recovery of such biomolecules in an active state is technically difficult, often requiring expensive downstream processing and leading to secondary pollution [2]. With the increasing pressure to develop environmentally friendly technologies, immobilization of enzymes onto solid support materials offers a better technological alternative.

Despite reports of lower catalytic activity of immobilized enzymes compared with the free (suspended) ones, overall, immobilization enhances the stability of the enzyme, and facilitates the easy separation and reuse of the active enzyme [2-6]. This enables better control over the reaction and eliminates additional costly downstream processing for product recovery. Usually, the immobilization step is very crucial because if the surface groups at the active site of the enzyme change their location or are involved in the reaction with the support, the catalytic activity can be lost [1]. Therefore, the choice of support and appropriate immobilization method is important for obtaining a stable and active enzyme [7]. Among the immobilization methods used, bioconjugation is the most preferred because it involves the formation of a stable irreversible covalent bond between a solid substrate or probe of choice (cells or polymers) and enzyme molecules [8-10].

The hydrolysis of urea to ammonia and carbon dioxide, catalysed by urease (EC 3.5.1.5), is a crucial reaction for the ecosystem. It is an important source of nitrogen for cellular growth (plant fertilization) [11], and it allows biomineralization for invertebrates via formation of calcium carbonate from carbon dioxide [12]. Therefore, the immobilization of urease has been extensively exploited in biomimetic field, like diagnostic tests for blood urea, in the construction of artificial kidneys, in biosensors, in the treatment of urea-containing effluents, in closed loop water circulation system in spaceships, calcium carbonate vesicles, insecticides and as a source of gas for rubber muscle actuators [6, 13-15]. Because urease immobilization enables repeated use of the

enzyme, thereby lowering the overall operating costs, new immobilization supports are still being sought by many researchers [3, 16].

Recently, there is wide interest in the immobilization of enzymes in a variety of mesoporous matrices, mostly for sensing or clinical analytical applications [1, 3, 4, 9, 15, 17]. For instance, Wang and Caruso [18] immobilized a range of enzymes with different molecular sizes in mesoporous silica spheres followed by encapsulation. Similarly, Azioune et al. [19] successfully prepared ester-functionalized polypyrrole-silica composite particles as bioadsorbents of human serum albumin. Of particular interest for such supports are the nitrogen-containing conjugated polymers and their composites because they offer direct electron transfer between the enzyme and support [6, 20]. Among the conjugated polymers, polypyrrole (PPy) has been the most investigated due to its non-toxicity, high chemical stability and excellent biocompatibility. Moreover, the easy synthesis of PPy in aqueous solution and simple functionalization with specific groups makes it suitable for the covalent attachment of biomolecules [21, 22]. In such systems with enzyme-loaded moieties, effective diffusion of the substrate into the pores of the support is a crucial step for interaction with the enzyme [4]. A common problem encountered in the use of such mesoporous materials is poor diffusion, resulting either from pore blockage by the immobilized enzyme, or by non-homogenous distribution of the enzyme, which is associated with low porosity and inaccessible specific surface area [23, 24]. A typical case is the immobilization of urease on a PANI/MWCNT hybrid, instead of being uniformly distributed within the entire polymer, urease was bound exclusively to the outer polymer surface. This was associated with the large size of urease compared with the pore size of the polymer [20]. Because of their small pore sizes, mesoporous materials have been generally restricted to the immobilization of enzymes with relatively small sizes [18].

Macroporous materials thus appear to be promising as robust chemically- and mechanically-stable platforms for enzyme immobilization leading to improved mass transport and performance of the enzyme. Çelebi et al. [17] prepared monoliths by copolymerization of glycidyl methacrylate

and ethylene dimethacrylate in a fused silica capillary and compared this with monodisperse porous poly (GMA-co-EDM) beads. They reported superior activity of the macroporous monolithic immobilized enzyme reactors compared with single particle-based supports, attributing this to convective diffusion in the macropores of the monolith. Similarly, Wang and Caruso [18] reported faster immobilization rates and improved immobilization capacity on mesoporous silica supports with larger pores. Despite reports about improved performance of porous nanostructures in comparison with bulk materials, many of the support materials applied for the immobilization of urease as a model enzyme have been in the form of particles and films, mainly for sensing and analytic applications [6, 16, 25-28]. For example, dendritic polypyrrole silver nanocomposite were prepared in the form of aggregates. This nanocomposite was subsequently dissolved and deposited as a polymer film onto which urease was immobilized for the development of a urea biosensor [29]. Similarly, Prissanaroon et al. [30] prepared a PPy film onto which urease was immobilized by physical adsorption and again applied as a potentiometric urea biosensor. Urease covalent immobilization on macroporous PPy support layer was investigated by Massafra et al. [31] but the macroporous structure was achieved by dissolution of polystyrene co-support forming macropores. To our best knowledge, the use of a carboxyl-functionalized 3D macroporous PPy prepared by a porogen-free method as a support for the covalent immobilization of urease has not yet been widely investigated.

In this work, we developed 3D macroporous materials bearing COOH groups using a simple approach and this material has been applied for the covalent immobilization of urease. Due to the rigid nanoparticle building blocks, these materials possess large, well-interconnected channels that enable easy accessibility to the active sites when serving as catalyst supports and allow for the immobilization of large biomolecules. We believe that such macroporous materials could help in reducing the diffusion resistance encountered during mass transfer and in addition facilitate easy separation of the enzyme from the reaction mixture by simple filtration. Moreover, for many of the matrices used, low loading capacity is associated with low number of sites for attachment due to

steric hindrance effect during the polymerization of bulky functionalized monomers. We rather employed polymerization of the COOH functionalized monomer and attach the enzyme directly after activation. The successful chemical modifications were confirmed using a combination of analytical techniques as described in Section 2.4. The immobilized enzymes showed high activity in the hydrolysis of urea coupled with high stability and reusability. The obtained 3D macroporous materials appear to have considerable potential as catalyst supports for a wide range of biomolecules.

2 Materials and Methods

Pyrrole, 1-(2-cyanoethyl) pyrrole monomers, KOH, HCl and all other chemicals were obtained from Sigma Aldrich. Polyvinylpyrrolidone (PVP-40, average molecular weight: 40000 g mol⁻¹) was used as stabilizer both in the preparation of the template nanoparticles and the 3D macroporous materials; iron (III) chloride hexahydrate (FeCl₃.6H₂O) was used as initiator. N-hydroxysulfosuccinimide (NHS) and N-Ethyl-N'-(3-dimethylaminopropyl) carbodiimide hydrochloride (EDC-HCl) were used for surface COOH activation. Urea and urease from *Canavalia ensiformis* (Jack bean, Type III lyophilized powder with activity of 34 150 units/g solid) was used in the concentration 0.44mg/ml for all immobilization experiments. Mixture of Na₂HPO₄ and NaH₂PO₄ were used as phosphate buffer pH=7.8. Nessler's reagent (K₂[HgI₄]) was used as ammonia indicator. Apart from pyrrole monomer which was freshly distilled before use, all other chemicals were used without modification or purification. For all solutions, deionized water with conductivity below 1 μS_{cm}-1 was used.

2.1 Preparation of the polypyrrole nanoparticles (PPy NPs)

Monodisperse PPy nanoparticles of 114 nm in diameter were synthesized according to Woo et al.[\[32\]](#) with slight modifications. PVP was dissolved in DI water (1 wt.%) followed by the

dissolution of $\text{FeCl}_3 \cdot 6\text{H}_2\text{O}$ into this solution. The mixture was kept under stirring for 2 hours and during this period, the mixture was purged with nitrogen. The solution was then cooled ($0 - 10^\circ\text{C}$) using an ice water bath. Freshly distilled pyrrole monomer was subsequently added and the polymerization was carried out for at least 10 hours under magnetic stirring at 400 rpm. The resulting latex was purified by centrifugation of latex/acetone mixture (1:1) per volume at 20000 rpm and redispersed in distilled water using PVP (latex/PVP = 6).

2.2 Preparation of the 1-(2-carboxyethyl) pyrrole monomer (Py-COOH)

The monomer 1-(2-carboxyethyl)pyrrole was synthesized according to the previously described procedures [19, 33] with slight modifications. First, 1-(2-cyanoethyl)-pyrrole (Aldrich) was hydrolyzed to 1-(2-carboxyethylpyrrole) by the addition of 11.92 mL of 1-(2-cyanoethyl)-pyrrole to 60 mL of KOH (6.7 M) under nitrogen. This mixture was then heated to reflux under an inert atmosphere until a red solution was obtained. After 2 h, the disappearance of the ammonia was confirmed using litmus paper. The solution was acidified to pH 5 using 8 M HCl at room temperature. The resulting product was extracted five times with diethyl ether while maintaining the solution at pH 5. After evaporation of the diethyl ether using a rotary evaporator, the resulting oil became a beige solid after cooling overnight at room temperature. The crude product was recrystallized from boiling n-heptane. After removal of the solvent, white “needle-like” crystals were formed, which were dried under a vacuum. The structure of this product was confirmed by NMR and FTIR spectroscopy, which were in agreement with the literature and commercial product. The synthetic steps, ^1H NMR and ^{13}C NMR spectra are shown in Figures SI 1, 2 and 3, respectively in the Supporting Information. The NMR peaks are also summarized in Table SI 1 also in Supporting Information.

2.3 Preparation of the 3D macroporous materials by coating PPy NPs with Py-COOH

To produce the 3D macroporous PPy bearing COOH groups on the surface (namely PPy-COOH/PPy NP), carboxylic acid functionalized pyrrole was dissolved in freshly distilled pyrrole (1:1). FeCl₃.6H₂O was dissolved in the latex solution (aqueous dispersion of PPy NPs) and stirred under N₂ atmosphere for 20 minutes with no visible aggregation. The Py-COOH/Py mixture was added as a shot using a syringe and the polymerization was allowed to run overnight with a stirring rate of 200 rpm resulting in the 3D microclusters. To increase the mechanical stability of the produced porous material, phytic acid was used as a crosslinker (polymer/crosslinker=1:1 wt.) resulting in the crosslinked material, xPPy-COOH/PPy NP. For comparison, macroporous materials were prepared without the carboxylic acid functionalities (namely PPy/PPy NP), where pyrrole was polymerized onto the surface of the PPy NPs. The aggregates were washed either by leaving the suspension to sediment or by filtration and the liquid decanted and replaced with fresh distilled water several times until the filtrate became clear. The prepared materials were characterized by a combination of analytical techniques.

2.4 Characterization of PPy NPs and macroporous materials

The surface morphology and structural properties of the PPy NPs and macroporous materials were characterized using a Mira 3 LMH Tescan scanning electron microscope. The size distribution of the PPy nanoparticles were measured with a diluted aqueous dispersion by dynamic light scattering (Malvern Zetasizer Nano Z). UV-vis absorbance spectrum of PPy NP suspension was recorded on a Shimadzu UV-2550 UV-visible-NIR spectrophotometer using a quartz cuvette with an optical path of 10 mm. The internal structures of porous materials was evaluated by determination of fractal dimension from static light scattering (Malvern, Mastersizer 2000) measurements. Surface areas of the macroporous materials were determined by measuring nitrogen adsorption on a Quantachrome Nova 2200e surface area analyser and evaluation using the BET

theory. Surface functionalities were confirmed by ATR-FTIR using a Nicolet iZ10 Spectrometer from 4000 cm^{-1} to 400 cm^{-1} and the spectra are an average of 64 scans. An Elementar vario EL Cube analyser (Germany) was used to measure the elemental composition of the samples whereas XPS measurements were conducted on Omicron Nanotechnology (monochrome, constant analyser mode) to confirm the surface functionalities. To confirm the successful immobilization of urease, elemental analysis and XPS were employed to evaluate the surface properties of the aggregates.

2.5 Immobilization of urease and activity tests

Urease was covalently attached to the functionalized 3D macroporous materials via a carbodiimine activation of surface groups. In order to activate the carboxyl groups on the surface of macroporous material, about 200 mg of wet porous aggregates (corresponding to 50 mg dry solid, assessed by desiccation of wet solid) was placed in a 0.1 M phosphate buffer (pH 7.8) containing 7.4mM NHS and 10mM EDC for 24 hours. The suspension was filtered to separate the activated particles. After rinsing with DI water, the activated support was placed in 5ml of urease solution (15 units/mL) dissolved in 0.1 M freshly prepared phosphate buffer with pH = 7.8 at 4-8 °C for 5 hr with stirring and 19 hours without stirring in order to form covalent bonds. After the immobilization step, the suspension was filtered and the immobilized enzyme washed 3 times with DI water to remove the unattached urease and then with phosphate buffer. This step was also performed after each measurement in reusability tests. For comparison, a blank sample was prepared by immobilizing urease on PPy-coated PPy NPs, non-functionalized particles and without any activation prior to enzyme incubation such that the enzyme is attached only by physical adsorption.

The activity of free urease was assessed by continuous formation of yellow precipitate of $(\text{NH}_4)_2[\text{HgI}_4]$ from addition of 350 μl of Nessler's reagent into 2.5ml urea-urease phosphate buffer solution while being stirred (800rpm) continuously for 900 seconds and measured at 480nm at 30°C [Ramesh 2011] on UV-Vis spectrophotometer Agilent 8454. After addition of Nessler's

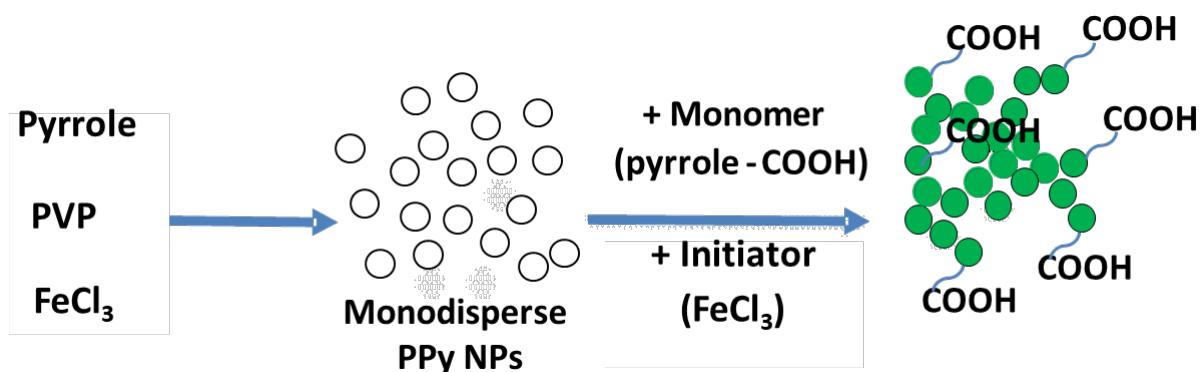
reagent, the initial concentration of urea was 123 mM, and concentration of phosphate buffer at pH 7.8 was 87.5 mM. The pH of phosphate buffer was chosen to avoid urease inhibition by phosphate buffer at pH lower than 7.5 [34]. Urease concentration was varied for each experiment creating a reference table of first derivations of absorbance (see Figure SI 4 in Supporting Information), and consequently used to evaluate the urease concentration in units per ml according to Jack bean urease bottle specifications. Please note that according to the specification, one unit of urease liberates 1 μ mol of NH_3 from urea in one minute at pH=7.0 at 25°C.

The performance of each sample of immobilized enzyme was measured by placing each sample on Spectra/PorTM MWCO:1000 membrane sheet, which was packed and placed into the stirred, heated and measured cuvette. The solution inside each cuvette consist of 2.5ml 87.5mM phosphate buffer pH=7.8, 350 μ l of Nessler's reagent and 123mM urea. Sample was continuously stirred (800rpm), heated to 30°C and measured at 480nm wavelength in UV-Vis spectrophotometer.

3 Results and discussion

3.1 Preparation of 3-D macroporous supports

The immobilization of enzymes onto a suitable support is the crucial step that determines the stability, structure and performance of the resulting immobilized enzyme [20]. Support materials bearing surface functionalities that enhance the covalent interaction with enzymes provide a feasible route for the attachment of stable enzymes. In this study, 3D macroporous supports bearing COOH groups were simply prepared and activated via carbodiimide chemistry, which enables the covalent attachment of urease. The material preparation was done in two steps (Scheme 1). First, PVP stabilized PPy NPs were synthesized. In the second step, Py-COOH was polymerized in aqueous medium in the presence of the PPy NPs resulting in a 3D structure with the particle blocks having a coating of PPy-COOH on the surface.



Scheme 1. Synthetic approach to 3D macroporous enzyme supports

The aqueous dispersion of the PPy NPs exhibits a strong black colour (see inset in Figure SI 5 in Supplementary Information) and the dispersion was highly stable when stored at room temperature for several months. The formation of the PPy NPs was further confirmed by UV-Vis spectroscopy (Figure SI 5 in Supplementary Information), with the nanoparticles exhibiting UV absorption between 300 – 600 and peaking at 470 nm. The observed spectrum corresponds to those reported previously for PPy NPs [35].

3.2 Morphological characterization of 3-D macroporous supports

Preparation of the PVP-stabilized PPy NPs was well controlled, as evidenced by the spherical and monodisperse particles obtained by SEM (Figure 1 (a)) with an average particle diameter of 114 ± 0.16 nm as determined by DLS.

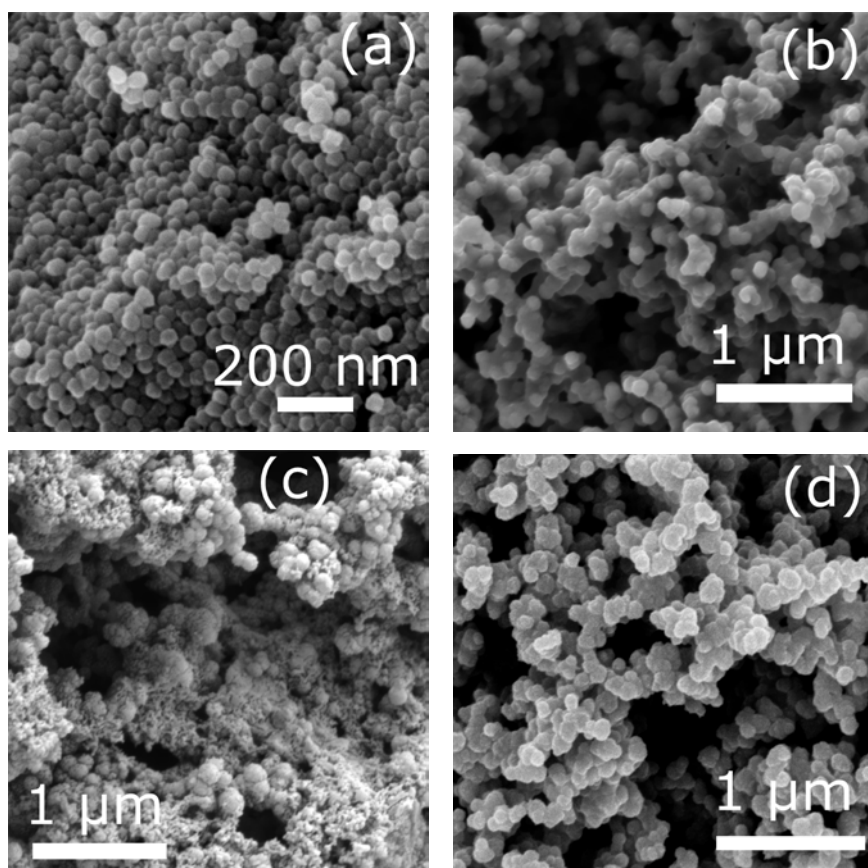


Figure 1. SEM images of (a) PPy NPs (b) PPy-COOH/PPy NPs (c) xPPy-COOH/PPy NPs (d) PPy/PPy NPs

After coating of the functionalized polymer onto the PPy NPs, 3D structures were obtained with uniform coating on the PPy NPs structure (Figure 1 (b), (c), (d)). The formation of such large 3D structures is advantageous for easy separation of the immobilized enzyme by simple filtration. We have shown that, to obtain such 3D structures, the use of PVP to redisperse the nanoparticles after the washing step is crucial in stabilizing the nanoparticles and ensuring that the subsequent coating step is effective. This stabilization step was necessary because we observed the PPy NPs redispersed without PVP showed a broader size distribution and a shift to larger sizes, indicative of aggregation (Figure SI 6 (a), Supporting Information), which was in line with previous studies[32, 36] Moreover, the 3D materials prepared using these particles showed non-uniformity (Figure SI 6 (b), Supporting Information).

The measurement of the intensity of scattered light as a function of scattering wave vector q , was used to evaluate the size and internal structure of the formed aggregates. A double logarithmic plot of the average structure factor $\langle S(q) \rangle$ as a function of q (see Figure 2) gives two key characteristics about the aggregates: (i) size in the form of mean radius of gyration $\langle R_g \rangle$ and (ii) internal structure characterized by the fractal dimension (d_f). The $\langle R_g \rangle$ was extracted from the curve bending region (Guinier region) whereas the d_f was obtained from the slope of the power law region. The $\langle R_g \rangle$ of the PPy/PPy NPs aggregates was 41 μm while that of the xPPy-COOH/PPy NPs was 46 μm . In contrast, the size of aggregates PPy-COOH/PPy is significantly lower with $\langle R_g \rangle$ around 13 μm indicating that presence of carboxyl groups on pyrrole macromonomer yield aggregates with lower strength. This effect was corrected by the addition of phytic acid as crosslinker. Because the aggregates were formed by assembly of many nanoparticle units held together by the polymer coating, the fractal dimension (d_f) gives an indication about the compactness of the formed materials. It was observed that the sample xPPy-COOH/PPy NPs and PPy-COOH/PPy NPs exhibited comparable value of fractal dimension ($d_f = 2.5$) to that of PPy/PPy NPs ($d_f = 2.4$). These values are very comparable with those measured by Brand et al. [37] for aggregates prepared from partially destabilized polystyrene nanoparticles. In contrast, our values are significantly lower compared to those measured by Lamprou et al. [38] for macroporous aggregates prepared from fully destabilized polystyrene nanoparticle, where d_f around 2.7 were reported. These results indicate that internal morphology of prepared aggregates is comparable to that prepared under partially destabilized conditions even though aggregation of PPy NPs in our case was induced by the precipitation of PPy on the surface of PPy NPs and not by the reduction of repulsive forces between primary particles.

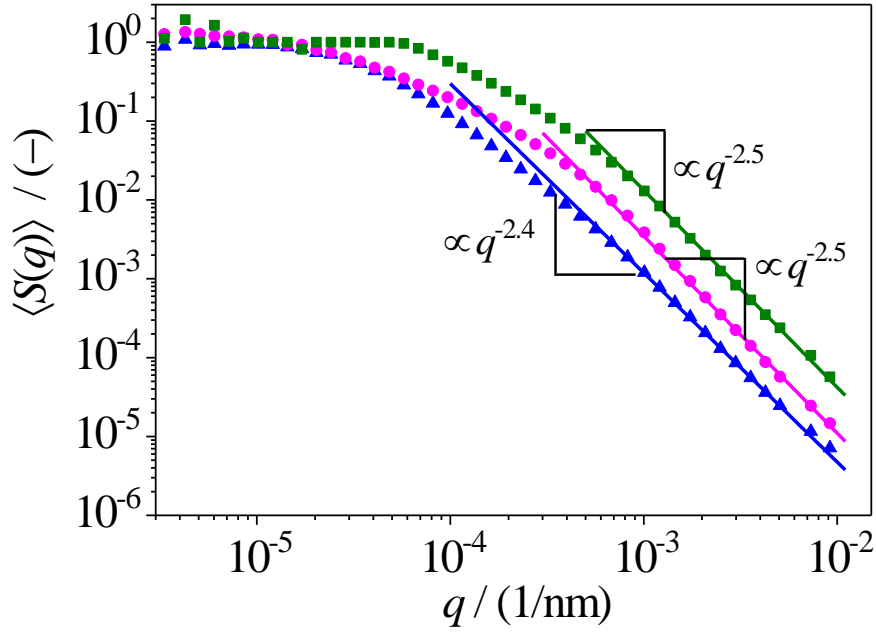


Figure 2. Double logarithmic plot $\langle S(q) \rangle$ vs. q used to determine $\langle R_g \rangle$ and d_f for prepared aggregates. (circles) xPPy-COOH/PPy NPs, (square) PPy-COOH/PPy NPs and (triangles) PPy/PPy NPs

3.3 Characterization of surface coating by FTIR spectroscopy

The successful preparation of the COOH-functionalized pyrrole monomer and formation of the Py-COOH-coated PPy NPs was monitored by FTIR spectroscopy as depicted in (Figure 3 (a)-(d)). The absence of N-H stretching vibrations in the spectrum of Py-COOH confirmed successful attachment of a COOH-terminated group to the N position of the pyrrole ring, also corresponds to spectra from the commercial product (Figure 3 (c)). All the aggregates showed characteristic peaks corresponding to the stretching vibrations (1544 and 1450 cm^{-1}) of the pyrrole ring. Weak absorption peaks at 1653 cm^{-1} , characteristic for the carbonyl group of PVP were observed for both samples, which is probably due to the residues of PVP in the material after washing. In addition, the weak peak at 1708 cm^{-1} in the spectrum of PPy NPs/Py-COOH is attributed to the carbonyl group of $-\text{COOH}$, thereby confirming that PPy-COOH had been successfully coated onto the PPy NP surface to form COOH-functionalized macroporous supports. This band was absent in the

spectrum of the PPy-coated PPy NPs. The broad peak ranging from 3500 to 1800 cm^{-1} indicated the presence of both OH groups from the carboxylic acid group (which occur around 3000 cm^{-1}) and presence of NH groups (which occur at 3400 cm^{-1}). A detailed description of the spectrum of precursors as well as a summary of the main peaks observed is presented in Section SI 1 and Table S2 in Supporting Information, respectively. These results are in line with several reports in the literature [39-41].

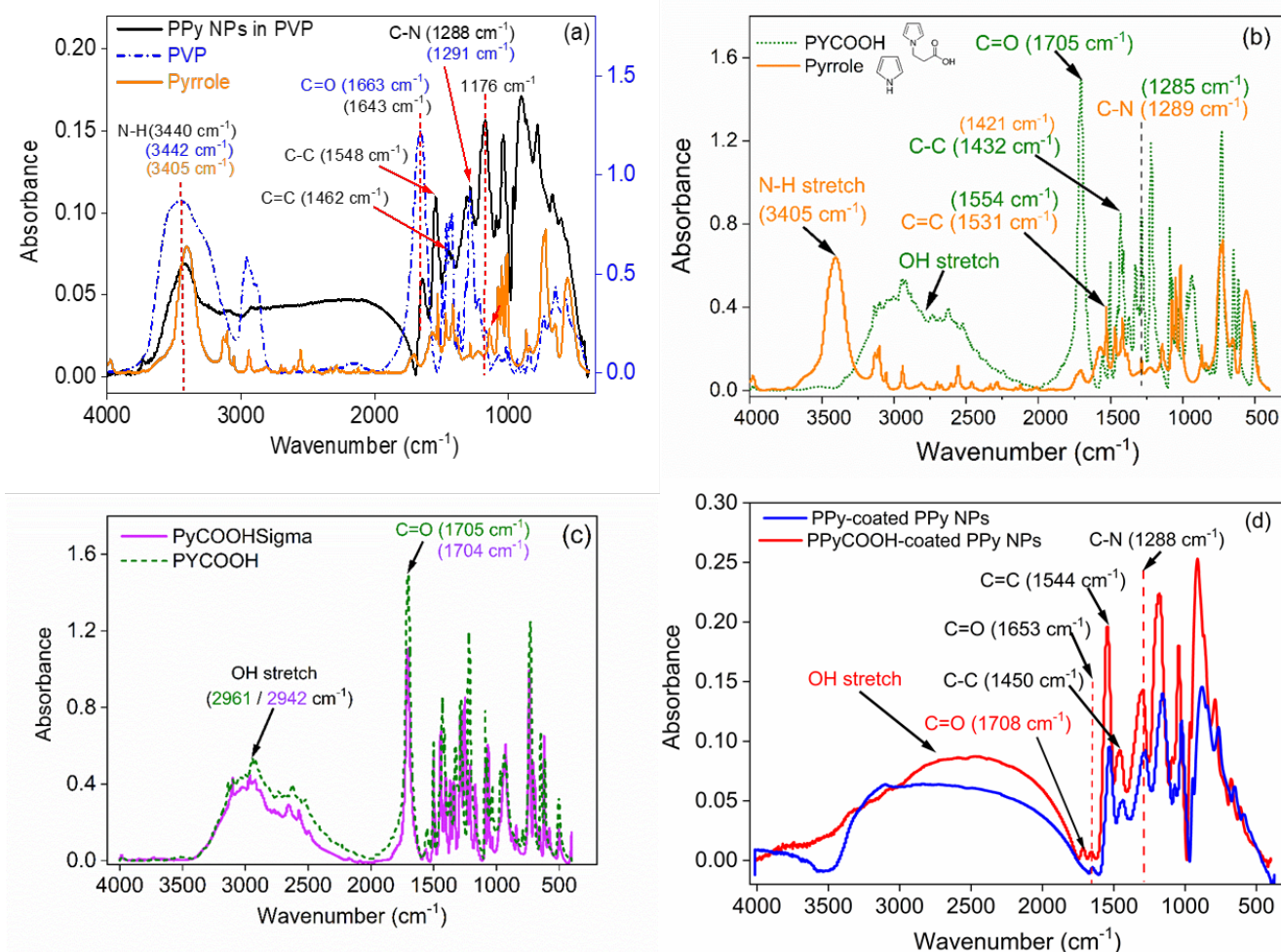


Figure 3. (a, b, c, d) FTIR spectra of the materials

3.4 Bulk composition by organic elemental analysis

Quantitative information about the composition was obtained from organic elemental analysis. The obtained results (Table 1) revealed an increase in oxygen amount from 25% in PPy NPs stabilized by PVP to 32% in PPy-COOH coated PPy NPs whereas the crosslinked material increased up to 62 %. This increase, which is due to contributions from COOH and phytic acid groups, was simultaneously accompanied by a decrease in the nitrogen content. Conversely, the control material coated with PPy alone exhibited the exact opposite effect. As the N content increased due to PPy coating, the oxygen content decreased from 25% in the PPy NPs to 21% in the PPy-coated particles. Overall, a decrease in carbon, nitrogen and hydrogen and a corresponding increase in oxygen content was observed after the coating. This increase in oxygen content corresponds to the polymerization of the carboxylic acid functionalized pyrrole monomer onto the PPy NPs and oxygen groups from phytic acid in the case of the crosslinked material. Since the crosslinked material recorded the most remarkable surface properties, it was chosen for subsequent analysis and enzyme immobilization. In order to study the nature of the surface functionalities, XPS was performed on the materials.

Table 1. Organic Elemental Analysis

Sample ID	Nitrogen	Carbon	Hydrogen	Oxygen ^a
PPy NPs	12.33 ± 0.038	55.91 ± 0.002	7.05 ± 0.002	24.71
PPy-COOH/PPy NPs	12.58 ± 0.023	50.83 ± 0.087	4.33 ± 0.005	32.27
xPPy-COOH/PPy NPs	6.21 ± 0.008	28.28 ± 0.003	3.43 ± 0.004	62.087
PPy/PPy NPs	15.50 ± 0.003	59.14 ± 0.003	4.54 ± 0.020	20.812

^a Calculated as follows: 100 % – (Nitrogen + Carbon + Hydrogen) %

3.5 Surface composition by X-ray photo spectroscopy (XPS)

The surface compositions of the materials were analyzed in more detail by XPS analysis as a useful way of interpreting the chemical modifications. The survey scans (Figure SI 6, (a) and (b)) exhibit C1s, N1s, O1s centered at 285, 399, 532 eV, respectively. In addition, Cl 2p (198 eV) and Fe 2p (716 eV) present in some of the materials (see summary in Table 2) could be indicative of the residues from the oxidizing agent (FeCl_3) used for preparing the materials. Moreover, a weak peak at 140 eV (Figure SI 6 (b)) is attributed to phosphorus from the crosslinking agent phytic acid. It was observed that ~~that~~ the oxygen content of the PPy-COOH coated materials increased as compared with the initial PPy NPs, with a corresponding decrease in nitrogen content (Table 2). When compared with the material coated with non-functionalized PPy, the chemical composition of these non-functionalized aggregates was almost similar to that of the PPy NPs. It is important to note that the nitrogen content of xPPy-COOH/PPy NPs decreased to 1.32 wt. % compared with 11 wt. % in the original PPy NPs. This confirms the successful coating of the xPPy-COOH onto the surface of the PPy NPs. The compositions obtained from XPS analysis were slightly lower than those obtained from organic elemental analysis. The differences are due to the fact that XPS takes into account only the surface composition whereas elemental analysis considers the bulk composition. For the sample xPPy-COOH/PPy NPs for instance, which contains the highest amount of oxygen, the amount recorded in XPS analysis was 38% whereas 62 % was recorded from organic elemental analysis.

Because of the interest in the carboxyl groups on the surface of the materials for further immobilization, detailed information about the carbon types on the surface was obtained by deconvolution of the C1s spectra. The deconvoluted C1s spectra of the PPy NPs and the composite (Figure SI 6 (c) and (d)) were fitted into five main groups C-C (284.6 eV), C-N (285.6 eV), C-O or charging effect (286.9 eV), C=O (287.9 eV) and COO (288.9 eV). The PPy NPs showed all four groups except -COO whereas the PPy-COOH/PPy NPs similarly showed all four peaks except the

one corresponding to C=O, which comes from PVP. The observed results are consistent with that of FTIR and organic elemental analysis.

Table 2 Summary of surface composition of the materials from XPS analysis

Sample ID	Carbon C1s % (Pos. 284.68)	Oxygen O1s % (Pos. 532.28)	Nitrogen N1s % (Pos. 399.35)	Chloro 2p % (Pos. 198.35)	Iron 2p % (Pos. 715.96)
PPy NPs	76.94	10.42	11.22	1.42	ND**
PPy- COOH/PPy NPs	69.38	19.49	7.56	2.94	0.64
xPPy- COOH/PPy NPs	56.32	37.59	1.32	3.50	1.27
PPy/PPy NPs	76.58	10.08	11.67	1.68	ND**
C1s deconvoluted peaks					
	C-C	C-N	C=O	COOH	C-O / Charging
PPy NPs	68.06	16.81	4.95	-	10.18
PPy- COOH/PPy NPs	53.94	17.29	11.72	4.68	12.37
xPPy- COOH/PPy NPs	49.63	11.92	ND**	23.38	15.07
PPy/PPy NPs	65.00	17.19	9.25	5.93	2.63

3.6 Textural properties

In addition to the presence of the surface functionalities, the porous properties of the aggregates also play an important role in their performance. This is particularly crucial for the application where the materials are being tested, e.g. in enzyme immobilization for catalysis. The material showed a typical type II adsorption isotherm according to the Bruner-Deming-Deming-

Teller classification, which is characteristic of macroporous structures (Figure 4 (a)). The size distribution of the pores Figure 4 (b) was evaluated using the density functional theory (DFT) from the N₂ adsorption isotherm. Although SEM images revealed mostly large macropores, these could not be characterized by N₂ sorption.

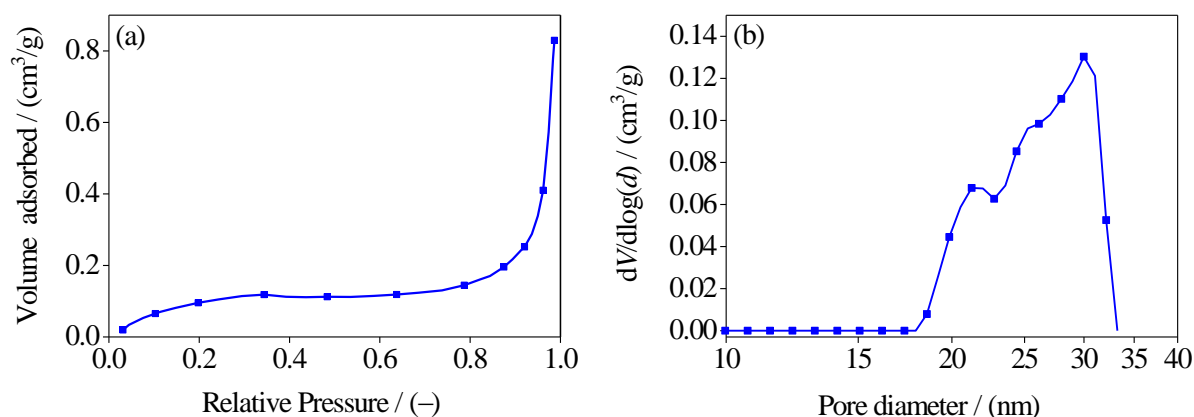


Figure 4. (a) Nitrogen adsorption isotherm of PPy/PPy-COOH (1:1) sample porous materials (b) differential pore size distribution from N₂ sorption data.

Mercury porosimetry was employed to confirm the high porosity of the obtained materials, similar to materials prepared using a similar approach [42, 43]. For catalytic reactions, easy access of the reactants to the active site of the enzyme is prerequisite to good performance, as such; larger pores in the material will provide the advantage of easy diffusion and mass transport. The presence of macropores in the prepared macroporous materials was confirmed by mercury porosimetry. A plot of intruded volume (cumulative pore volume) vs pressure (Figure 5a) revealed a continuous increase in mercury uptake with increase in Hg intrusion pressure until a saturation was reached. This indicates that the materials possess a very large macropore volume with high porosities of up to 93%. Both non-crosslinked materials showed a double PSD (Figure 5b), which can be distinguished by intrusion of mercury between the particles and intra-particle porosity where mercury intrudes the smaller pores at higher pressure. The PSD for the crosslinked material xPPy-COOH/PPy NPs (Figure 5c) on the other hand showed one broad peak, and was characterized by a slightly lower porosity which was in the order of 79.3 %, compared to the non-crosslinked

materials. Due to its high content of COOH groups which is essential for the enzyme immobilization application, this material was selected as the enzyme support.

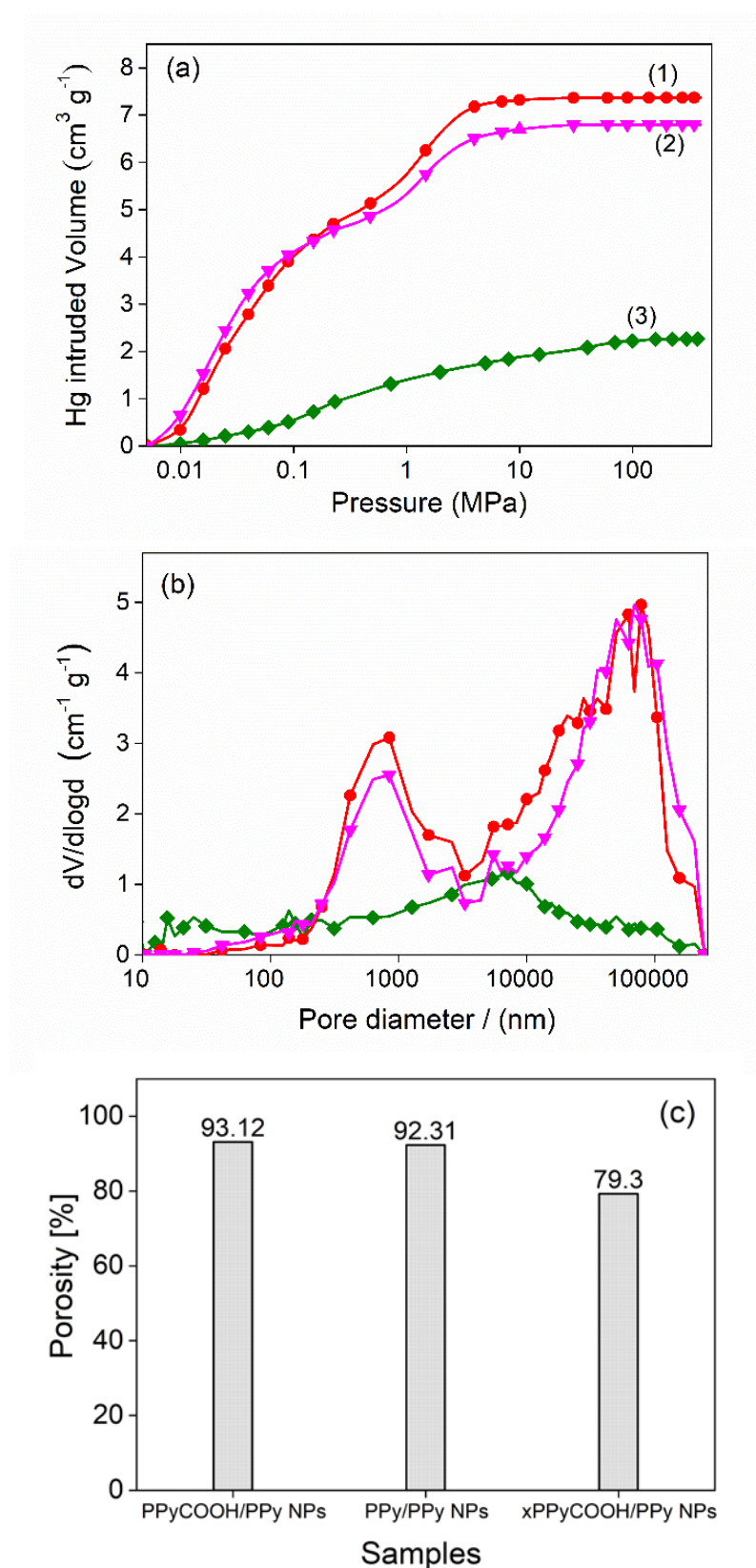
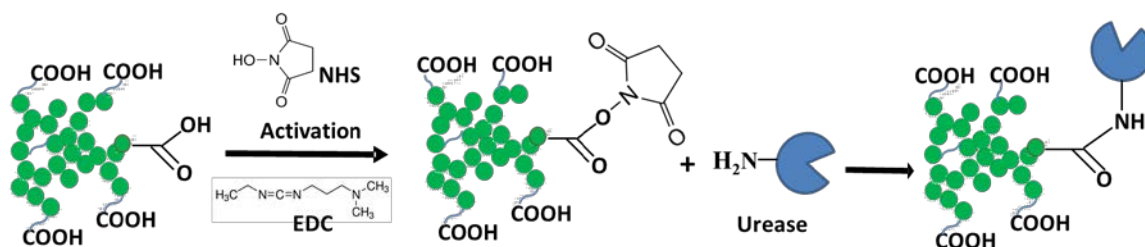


Figure 5. (a) Mercury intrusion isotherm of (1) PPy-COOH/PPy NPs (2) PPy/PPy NPs (3) xPPy-COOH/PPy NPs, (b) corresponding pore size distributions and (c) material porosity

3.7 Immobilization of Urease onto 3D xPPyCOOH/PPy

The 3D xPPy-COOH/PPy macroporous material was evaluated as a bioadsorbent for urease. The surface COOH groups were activated by adding of a coupling agent N-hydroxysuccinimide in the presence of carbodiimide (NHS/EDC) followed by covalent bonding of urease. The chemical reaction leading to the covalent attachment of the enzyme is depicted in Scheme 2. The NHS group reacts with the enzyme, forming an amide bond. As suggested by Azioune et al. [19], a similar covalent reaction has been associated with the chemical reaction between amino groups of protein and the pendent ester groups of the functionalized support. Although urease can also be attached to polypyrrole surface through strong hydrophobic or electrostatic interactions [44], [45], it may not yield a stable enzyme for repeated application. Thus, this study specifically incorporated COOH groups on the support (that can be easily modified using coupling agents), which formed covalent bonds with urease. It is important to note that due to the presence of phytic acid crosslinker and residues of PVP as detected by XPS and IR analysis, respectively, there may be physical adsorption of the enzyme through hydrogen bonding. However, enzyme activity tests with crosslinked supports which were not treated with the coupling agents, showed almost no activity, confirming minimal physical adsorption of the enzyme onto the supports. Due to the unique physicochemical properties and ease of functionalization of the conjugated polymer, polypyrrole [22], the support material showed good affinity to the enzyme. PPy coated onto PPy NPs was used as a non-covalent/covalent comparison for urease attachment performance and endurance.



Scheme 2. Reaction steps for the covalent attachment of urease.

Organic elemental analysis confirmed the successful immobilization of the enzyme on the PPy-COOH support (see Figure 6). The increase in nitrogen content together with the simultaneous decrease in oxygen content clearly points to the incorporation of urease onto the xPPy-COOH/PPy NP support, which binds through the O groups coming from COOH and incorporates N groups from NH₂ on the enzyme. Moreover, the detection of sulphur in the immobilized urease support, which was absent in the composition of the non-modified support, and the increase in carbon content is a further indication of successful urease immobilization; this is because enzymes consist of amino acids that have sulphur present in them.

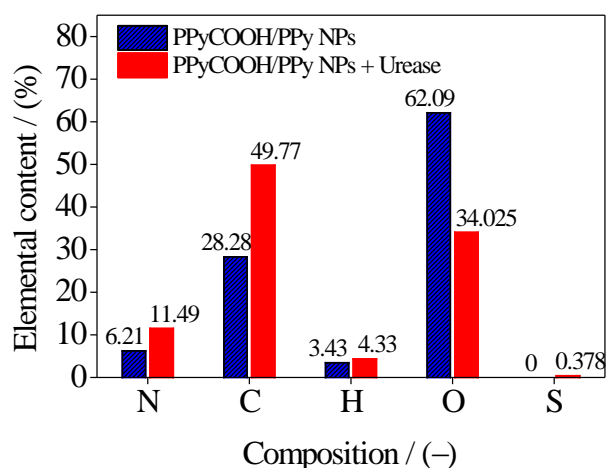


Figure 6. Elemental composition before and after urease immobilization

Comparison of FTIR and XPS spectra of the PPy-COOH-coated NPs before and after urease immobilization (see Figure 7) confirmed successful attachment of urease. The N-H stretching vibrations peaking at 3386 cm⁻¹, which are quite dominant after urease immobilization, is probably from amine groups of the immobilized enzyme (Figure 7 (a)). This peak is not visible in the PPy-COOH-coated NPs because the PPy-COOH monomer does not have the N-H peak (functionalization at this position, see also (Figure 3 (c))) and the absorption from PPy alone might be weak. Amide bond formation between the support and the enzyme urease was characterized by the disappearance of the acid group at 1708 cm⁻¹ and appearance of a shoulder peak at 1692 cm⁻¹.

In addition, the shift of C-C, C=C, – C-N and N-C vibrations from 1544, 1460, 1290 and 1176 cm^{-1} in PPy-COOH-coated NPs to higher wavenumbers 1561, 1475, 1320 and 1205 cm^{-1} , respectively, after immobilization further confirms the interaction between the support material and urease. We further confirmed the immobilization of urease onto the supports by comparing the XPS spectra before and after urease immobilization. The full spectrum scan (Figure 7 (b)) revealed an increase in the nitrogen content, which could come from urease immobilized on the material surface. These results are in line with the elemental analysis results (Figure 6).

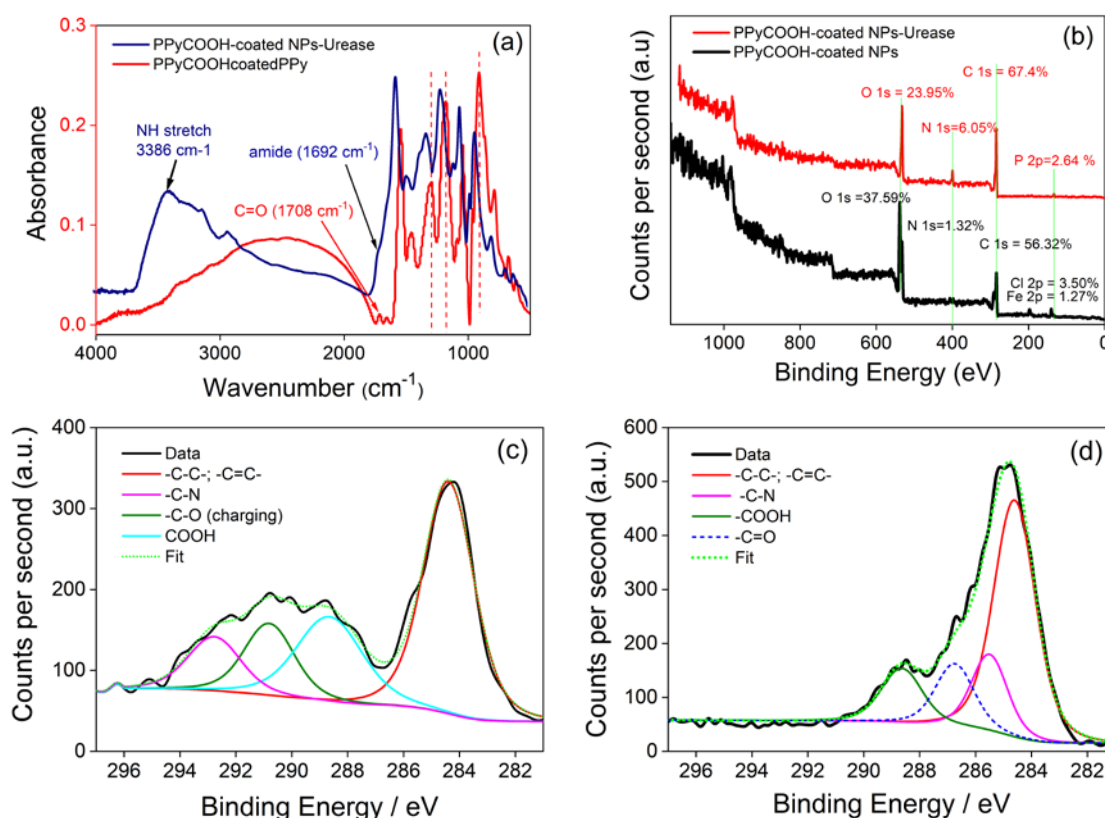


Figure 7. (a) FTIR and (b) full XPS spectra of support before and after urease immobilization (c),

C 1s peaks of xPPyCOOH/PPy NPs (d) C 1s peaks of xPPyCOOH/PPy NPs after urease immobilization

3.8 Activity, stability and reusability of the immobilized enzyme

To qualitatively evaluate the performance of immobilized urease we measured the amount of produced ammonia during urea hydrolysis. This was done by addition of Nessler's reagent

followed by a continuous monitoring of linear growth of absorbance at 480nm, which was used to evaluate the urease activity. All samples were loaded with the urease solution with the concentration of 15units/mL and were measured in the phosphate buffer with pH=7.8 at 30°C.

The comparison of the performance between covalently immobilized urease on xPPy-COOH/PPy NPs and non-covalent immobilization on PPy/PPy NPs is summarized in Figure 9 (a). As can be seen, the xPPy-COOH/PPy NPs-urease stationary phase reacts immediately after the start of the experiment, followed by the slowing down of the reaction which was observed after 400 seconds. PPy/PPy NP-urease stationary phase on the other hand starts to react approximately after 500 seconds followed by a linear growth. By comparing the first derivative of the growth period for these two experiments it was found that the performance of both materials is very similar resulting in an apparent activity of PPy-COOH-urease and of PPy-urease equal to 20 units/mL and 20.2 units/mL, respectively. When comparing the performance of covalently and non-covalently immobilization with respect to free urease we found an increase of about 33%. This is significantly higher than the one reported in the literature [46, 47] where an increase of only a few percent was reported. Furthermore, this increase is significantly higher than that measured for PPy support generated on the surface of electrode reported by Hosseini et al.[48] where there was a drop of activity of immobilized urease compared to the free enzyme, which is complete opposite to our observation.

Reusability experiments shown in Figure 9 (b) and (c) were performed to evaluate the capability of the stationary phase to preserve the enzyme activity. Each experiment was performed for 900 seconds followed by the filtration and washing of the sample 3 times with DI water as described above.

In Figure 9 (b), it can be seen that there is a significant drop in the enzyme activity after the second cycle of reusability of the PPy based stationary phase with non-covalently immobilized urease. In contrast, in the case of the covalently immobilized enzyme shown in Figure 9 (c) a delay was observed at the beginning of the reaction; however, the consequent time evolution of

absorbance is not significantly affected. This indicates that activity of the enzyme was preserved even though there is an increasing delay of the reaction startup, most probably caused by the deactivation of the small part of enzyme located on surface of the support. However, the small drop in the measured enzyme activity (less than 10%) suggests that most the enzyme is located in the pores of the stationary phase and thus protected against deactivation.

A further indication that the PPyCOOH based stationary phase with covalently bound enzyme outperformed the free enzyme and PPy based stationary phase with non-covalently bound enzyme is presented in Figure 9 (d). As can be seen, the covalently bound enzyme has significantly better time stability than the non-covalently bound enzyme over the complete testing period. In addition, the activity of the non-covalently bound enzyme drops to the level similar to that of the drop in activity of the free enzyme.

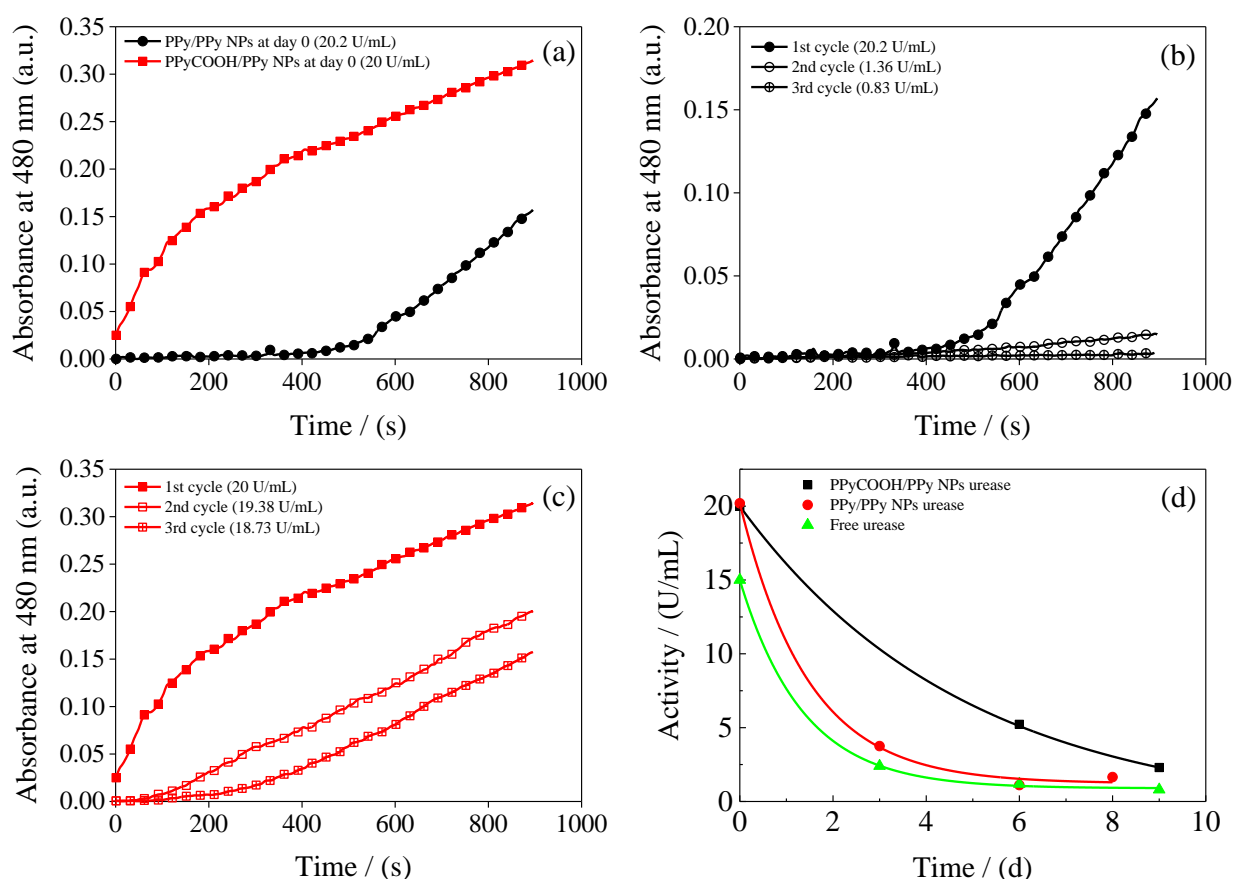


Figure 8 Time evolution of absorbance measured at 480nm for urease loaded support with urea in phosphate buffer pH=7.8 at 30°C after addition of Nessler's reagent. In brackets are indicated evaluated enzyme activities. a) The comparison of urea immobilized on PPy-COOH/PPy NPs and on PPy/PPy NPs support, b) example of reusability of immobilized urease on PPy/PPy NPs support, c) example of reusability of urease on PPy-COOH/PPy NPs support.

4 Conclusions

We have demonstrated a simple approach for the preparation of a 3D macroporous polypyrrole (PPy)-based material bearing COOH functional groups using PPy nanoparticles (NPs) as building blocks. The resulting materials have high porosities covering the range from 80 to 93 percent, with pore sizes covering the range from a few hundreds of nanometers up to tenths of microns. The material was successfully applied as support for urease enzyme immobilization. This was confirmed both by elemental analysis and by XPS. More importantly, it was found that covalent immobilization is capable of maintaining the 3D structure of the enzyme for repeated use. Such immobilized enzyme retained its full activity after three consecutive uses, which is advantageous compared to the free enzyme, which might be difficult to recover from the solution mixture. Furthermore, we confirmed long-term stability of covalently immobilized enzyme compared to the physically adsorbed and free enzyme systems. The easy synthesis approach, interesting physicochemical characteristics as well as the easy functionalization of PPyCOOH based 3D structure makes it a suitable support for enzymes or large biomolecules immobilization to be used for biocatalysis or as stationary phases for chromatography.

Acknowledgements: Financial support by a Czech Science Foundation (GACR) grant [16-22997S] and specific university research grants [MSMT No. 20/2017] and [MSMT No 21-

SVV/2018] are gratefully acknowledged. The authors are grateful to Anna Beltzung for helpful discussions, Antoine Klaue for SEM measurements and Stefano Caimi for NMR analysis.

5 References

- 1) Mishra, N., K. Pithawala, and A. Bahadur, Byssus thread: a novel support material for urease immobilization. *Appl Biochem Biotechnol*, 2011. 165(7-8): p. 1568-76.
- 2) Nguyen, H.H. and M. Kim, An overview of techniques in enzyme immobilization. *Appl. Sci. Conver. Technol.*, 2017. 26(6): p. 157-163.
- 3) Bartolini, M., V. Cavrini, and V. Andrisano, Choosing the right chromatographic support in making a new acetylcholinesterase-micro-immobilised enzyme reactor for drug discovery. *Journal of Chromatography A*, 2005. 1065(1): p. 135-144.
- 4) Benčina, M., et al., Immobilization of deoxyribonuclease via epoxy groups of methacrylate monoliths. *Journal of Chromatography A*, 2005. 1065(1): p. 83-91.
- 5) Datta, S., L.R. Christena, and Y.R. Rajaram, Enzyme immobilization: an overview on techniques and support materials. *3 Biotech*, 2013. 3(1): p. 1-9.
- 6) Laska, J., J. Włodarczyk, and W. Zaborska, Polyaniline as a support for urease immobilization. *Journal of Molecular Catalysis B: Enzymatic*, 1999. 6: p. 549-553.
- 7) Rafiq, K., et al., Fabrication of a highly effective electrochemical urea sensing platform based on urease-immobilized silk fibroin scaffold and aminated glassy carbon electrode. *Sensors and Actuators B: Chemical*, 2017. 251: p. 472-480.
- 8) Alatawi, F.S., M. Monier, and N.H. Elsayed, Amino functionalization of carboxymethyl cellulose for efficient immobilization of urease. *Int J Biol Macromol*, 2018. 114: p. 1018-1025.
- 9) Benčina, K., et al., Enzyme immobilization on epoxy- and 1,1'-carbonyldiimidazole-activated methacrylate-based monoliths. *Journal of Separation Science*, 2004. 27(10-11): p. 811-818.

- 10) Presolski, S.I., V.P. Hong, and M.G. Finn, Copper-Catalyzed Azide-Alkyne Click Chemistry for Bioconjugation. *Curr Protoc Chem Biol*, 2011. 3(4): p. 153-162.
- 11) Sigurdarson, J.J., S. Svane, and H. Karring, *The molecular processes of urea hydrolysis in relation to ammonia emissions from agriculture*. *Reviews in Environmental Science and Bio/Technology*, 2018. **17**(2): p. 241-258.
- 12) Wooldridge, S.A., *Mass extinctions past and present: a unifying hypothesis*. *Biogeosciences Discussions*, 2008. **5**: p. 2401-2423.
- 13) Gabrovska, K., et al., Immobilization of urease on nanostructured polymer membrane and preparation of urea amperometric biosensor. *Int J Biol Macromol*, 2011. 48(4): p. 620-6.
- 14) Kara, F., G. Demirel, and H. Tunturk, Immobilization of urease by using chitosan-alginate and poly(acrylamide-co-acrylic acid)/kappa-carrageenan supports. *Bioprocess Biosyst Eng*, 2006. 29(3): p. 207-11.
- 15) Selvamurugan, C., A. Lavanya, and B. Sivasankar, A comparative study on immobilization of urease on different matrices. *Journal of Scientific and Industrial Research*, 2007. 66: p. 655-659.
- 16) Zhou, J., et al., Preparation and property of urease immobilization with cationic poly(4-vinylpyridine) functionalized colloidal particles. *Chem. Biochem. Eng. Q.*, 2013. 27(4): p. 431-437.
- 17) Çelebi, B., A. Gökaltun, and A. Tuncel, Comparison of activity behaviors of particle based and monolithic immobilized enzyme reactors operated in semi-micro-liquid chromatography system. *Separation and Purification Technology*, 2013. 118: p. 294-299.
- 18) Wang, D. and F. Caruso, Mesoporous silica spheres as supports for enzyme immobilization and encapsulation. *Chem. Mater.*, 2005. 17: p. 953-961.
- 19) Azioune, A., et al., Synthesis and characterization of active ester-functionalized polypyrrole-silica nanoparticles: application to the covalent attachment of proteins. *Langmuir*, 2004. 20: p. 3350-3356.

- 20) Meibodi, A.S.E. and S. Haghjoo, Amperometric urea biosensor based on covalently immobilized urease on an electrochemically polymerized film of polyaniline containing MWCNTs. *Synthetic Metals*, 2014. 194: p. 1-6.
- 21) Jiang, H., et al., Poly(1-(2-carboxyethyl)pyrrole)/polypyrrole composite nanowires for glucose biosensor. *Electrochimica Acta*, 2012. 70: p. 278-285.
- 22) Liu, S., et al., Soft-Template Construction of 3D Macroporous Polypyrrole Scaffolds. *Small*, 2017. 13(14).
- 23) Albuszis, M., et al., Macroporous uniform azide- and alkyne-functional polymer microspheres with tuneable surface area: synthesis, in-depth characterization and click-modification. *Polym. Chem.*, 2014. 5(19): p. 5689-5699.
- 24) Kibarar, G. and G. Akovali, Optimization studies on the features of an activated charcoal-supported urease system. *Biomaterials*, 1996. 17: p. 1473-1479.
- 25) Rahmanian, R. and S.A. Mozaffari, Electrochemical fabrication of ZnO-polyvinyl alcohol nanostructured hybrid film for application to urea biosensor. *Sensors and Actuators B: Chemical*, 2015. 207: p. 772-781.
- 26) Sahoo, B., S.K. Sahu, and P. Pramanik, A novel method for the immobilization of urease on phosphonate grafted iron oxide nanoparticle. *Journal of Molecular Catalysis B: Enzymatic*, 2011. 69(3-4): p. 95-102.
- 27) Soni, A., R.K. Surana, and S.K. Jha, Smartphone based optical biosensor for the detection of urea in saliva. *Sensors and Actuators B: Chemical*, 2018. 269: p. 346-353.
- 28) Tetiker, A.T. and F. Ertan, Investigation of some properties of immobilized urease from *Cicer arietinum* and its using in determination of urea level in some animal feed. *Journal of Innovations in Pharmaceutical and Biological Sciences*, 2017. 4(2): p. 1-6.
- 29) Pandey, A.K., et al., Synthesis and characterization of dendritic polypyrrole silver nanocomposite and its application as a new urea biosensor. *Journal of Applied Polymer Science*, 2018. 135(3): p. 45705.

- 30) Prissanaroon-Ouajai, W., et al., Potentiometric Urea Biosensor Based on a Urease-Immobilized Polypyrrole. *Macromolecular Symposia*, 2015. 354(1): p. 334-339.
- 31) Massafra, M.P. and S.I.C. de Torresi, *Urea Amperometric Biosensors Based on Nanostructured Polypyrrole*. *Electroanalysis*, 2011. **23**(11): p. 2534-2540.
- 32) Woo, H.-Y., et al., Synthesis and dispersion of polypyrrole nanoparticles in polyvinylpyrrolidone emulsion. *Synthetic Metals*, 2010. 160(7-8): p. 588-591.
- 33) Maeda, S., R. Corradi, and S.P. Armes, Synthesis and characterization of carboxylic acid-functionalized polypyrrole-silica microparticles. *Macromolecules*, 1995. 28: p. 2905-2911.
- 34) Krajewska, B., *Ureases I. Functional, catalytic and kinetic properties: A review*. *Journal of Molecular Catalysis B: Enzymatic*, 2009. **59**(1-3): p. 9-21.
- 35) Chen, X., et al., Synthesis of polypyrrole nanoparticles for constructing full-polymer UV/NIR-shielding film. *RSC Advances*, 2015. 5(117): p. 96888-96895.
- 36) Armes, S.P. and M. Aldissi, Preparation and characterization of colloidal dispersions of polypyrrole using poly(2-vinyl pyridine)-based steric stabilizers. *Polymer*, 1989. 31.
- 37) Brand, B., M. Morbidelli, and M. Soos, Shear-Induced Reactive Gelation. *Langmuir*, 2015. 31(46): p. 12727-35.
- 38) Lamprou, A., et al., Synthesis of macroporous polymer particles using reactive gelation under shear. *Langmuir*, 2014. 30(23): p. 6946-53.
- 39) Bryaskova, R., et al., Synthesis and comparative study on the antimicrobial activity of hybrid materials based on silver nanoparticles (AgNps) stabilized by polyvinylpyrrolidone (PVP). *J Chem Biol*, 2011. 4(4): p. 185-91.
- 40) Cao, J., et al., Three-dimensional graphene oxide/polypyrrole composite electrodes fabricated by one-step electrodeposition for high performance supercapacitors. *Journal of Materials Chemistry A*, 2015. 3(27): p. 14445-14457.
- 41) Dubal, D.P., et al., Porous polypyrrole clusters prepared by electropolymerization for a high performance supercapacitor. *Journal of Materials Chemistry*, 2012. 22(7): p. 3044.

- 42) Kutorglo, E.M., et al., Nitrogen-rich hierarchically porous polyaniline-based adsorbents for carbon dioxide (CO₂) capture. *Chemical Engineering Journal*, 2019. 360: p. 1199-1212.
- 43) Kutorglo, E.M., et al., Synthesis of conductive macroporous composite polymeric materials using porogen-free method. *Colloids and Surfaces A: Physicochemical and Engineering Aspects*, 2018. 557: p. 137-145.
- 44) Yip, Y., et al., Interactions of reactive polypyrrole-coated polystyrene latex particles with gold nanoparticles and silanized glass. *Surface and Interface Analysis*, 2006. 38(4): p. 535-538.
- 45) Kim, H., et al., Urease adsorption immobilization on ionic liquid-like macroporous polymeric support. *Journal of Materials Science*, 2019. 54(24): p. 14884-14896.
- 46) Gambhir, A., et al., *Coimmobilization of urease and glutamate dehydrogenase in electrochemically prepared polypyrrole-polyvinyl sulfonate films*. *Applied Biochemistry and Biotechnology*, 2001. **96**(1): p. 249-257.
- 47) Gambhir, A., et al., *Covalent immobilization of urease on polypyrrole microspheres for application as a urea biosensor*. *e-Polymers*, 2002. **052**.
- 48) Hosseinian, M., G. Najafpour, and A. Rahimpour, *Amperometric urea biosensor based on immobilized urease on polypyrrole and macroporous polypyrrole modified Pt electrode*. *Turkish Journal of Chemistry*, 2019. **43**(4): p. 1063-1074.